

1 Water Vapor Retrieval using the Precision Solar Spectroradiometer

2
3 **Raptis Panagiotis-Ioannis^{1,2}, Kazadzis Stelios¹, Gröbner Julian¹, Kouremeti**
4 **Natalia¹, Doppler Lionel³, Becker Ralf³, Helmig Constantinos²**

5
6 ¹*Physikalisch-Meteorologisches Observatorium Davos-World Radiation Center (PMOD-WRC),*
7 *Davos, Switzerland*

8 ²*University of Athens, Department of Physics, Athens, Greece*

9 ³*Deutscher Wetterdienst, Meteorologisches Observatorium Lindenberg – Richard Assmann*
10 *Observatorium (DWD, MOL-RAO), Lindenberg (Tauche), Germany*

14 **Abstract.**

15 The Precision Solar SpectroRadiometer (PSR) is a new spectroradiometer developed at
16 Physikalisch-Meteorologisches Observatorium Davos-World Radiation Center (PMOD-WRC),
17 Davos, measuring Direct Solar Irradiance at the surface, in the 300-1020 nm spectral range at
18 high temporal resolution. The purpose of this work is to investigate the instrument's potential
19 of retrieving Integrated Water Vapor (IWV) using its spectral measurements. Two different
20 approaches were developed in order to retrieve IWV, the first one using single
21 channel/wavelength measurements, following a theoretical water vapor high absorption
22 wavelength, and the second one using direct sun irradiance integrated at a certain spectral
23 region. IWV results have been validated using a 2-year dataset, consisting of an AERONET sun-
24 photometer Cimel CE318, a Global Positioning System (GPS), a Microwave Radiometer
25 Profiler (MWP) and radiosonde retrievals recorded at Meteorological Observatorium
26 Lindenberg, Germany. For the monochromatic approach, better agreement with retrievals
27 from other methods/instruments was achieved using the 946nm channel, while for the
28 spectral approach using the 934-948 nm window. Compared to other instruments' retrievals,
29 the monochromatic approach leads to mean relative differences up to 3.3% with the
30 coefficient of determination (R^2) being in the region of 0.87-0.95, while for the spectral

1 approach mean relative differences up to 0.7% were recorded with R^2 in the region of 0.96-
2 0.98. Uncertainties related to IWV retrieval methods were investigated and found to be less
3 than 0.28cm for both methods. Absolute IWV deviations of differences between PSR and
4 other instruments were determined the range of 0.08-0.30 cm and only in extreme cases
5 would reach up to 15%.

6

7 **1.Introduction**

8 Water Vapor is a very important component of the thermodynamic state of the atmosphere
9 (Hartman et, al 2013), being a greenhouse gas with relatively high concentrations. The
10 quantity of water in the vapor state depends on temperature. So, from a climate change
11 perspective, it is considered as a feedback agent (Soden and Hled, 2006). Also, it is an
12 important component of the hydrological cycle and estimations of it are used in
13 meteorological forecast models (eg. Hong et al., 2015, Bock et al., 2016). Finally, a robust
14 estimation is needed to study microphysical processes that lead to the formation of clouds
15 and determine their composition (water droplets or ice crystals) as well as the statistical
16 shape and size of these components (Reichard et al., 1996, Yu et al., 2014).

17 IWV in the vertical atmospheric column is a very common variable in meteorological and
18 climatological studies. It is defined as the height that water would stand if completely
19 condensed and collected in a vessel of the same unit cross section (American Meteorological
20 Society, 2015). Monitoring of water vapor in the atmosphere has been performed through
21 radiosondes and provided through measurements of vertical profiles of humidity. These
22 measurements are limited to relatively infrequent (radiosonde) launches; thus, during the last
23 decades there have been developed methods to retrieve IWV from other devices:

- 24 • Continuous monitoring of IWV is established through Global Positioning System (GPS)
25 satellite observations (Bevis et al., 1992), which could be used to retrieve IWV
26 anywhere in the globe at relatively high temporal frequencies. The theoretical basis
27 for these measurement is that delays in the signals emitted by GPS satellites are
28 caused by the amount of water in the atmosphere, and through proper calibration,
29 such delays could be expressed as function of the IWV. Thus, as long as there are
30 ground based GPS receivers, after the appropriate post-processing of the received
31 signals, IWV can be retrieved.

- 1 • Microwave Radiometer Profilers (MWP) measure the emitted microwave radiation of
2 the atmosphere and retrieve water vapor vertical profiles and then IWV, providing
3 continuous data at very high frequencies under all weather conditions (e.g. Güldner
4 and Spankuch, 2001, Güldner, 2013). These instruments provide very high accuracy
5 but are not very common.
- 6 • Measurements from sun-photometers (eg CIMEL, PREDE-POM, MFR) have also been
7 used to calculate water vapor transmittance and, thus, estimate IWV. Filter
8 radiometer recordings in the spectral region around water vapor absorption bands, in
9 the near infrared region, are used to calculate this quantity (Halthore et al., 1997,
10 Campanelli et al., 2018, Nyeki et al., 2005). The World Meteorological Organization
11 (WMO) recommends the use of spectral windows centered around 719, 817 and 946
12 nm, though the most frequently used is the 946 nm bandpass, which Ingold et al.
13 (2000), showed that provides the most robust results.

14

15 Global networks of deployed sun-photometric devices are capable of providing IWV time
16 series. The AErosol RObotic NETwork (AERONET) retrieves IWV at more than five hundred
17 stations around the globe since the 1990's (Holben et al. 1998,
18 <https://aeronet.gsfc.nasa.gov/>) using the Cimel instrument. Other sun-photometers such as
19 the Precision Filter Radiometers (PFR) (Nyeki et al., 2005) have also been used by the Global
20 Atmosphere Watch (GAW) WMO program to monitor IWV. Furthermore, the SKYNET
21 radiometer network (details on: <http://atmos2.cr.chiba-u.jp/skyenet/>) also retrieves IWV using
22 Prede-POM sunphotometers at many stations (Campanelli et al., 2012, 2014). Finally, national
23 networks of sunphotometers are installed and operating in some countries also provide
24 Integrated Water Vapor (IWV) retrievals, eg. China Aerosol Remote Sensing NETwork
25 (CARSNET) is using the 936nm channel to provide IWV (Che et al., 2016).

26 Schneider et al. (2010) provided a very detailed comparison of different instrument retrievals
27 over a 4-year data set recorded at Izaña Atmospheric Observatory, Tenerife, Spain. They
28 found that MWP is the most precise technique and, in addition, it is independent of weather
29 conditions, while sun-photometric retrievals were limited by cloudy and biased by dry/humid
30 atmospheres, and GPS retrieved IWV showed deviations at lower IWV values. Deviations were
31 also recorded when compared to radiosondes, which was explained by the difference in air
32 masses and time scales among radiosondes and other IWV retrievals.

1 Technological advances of the recent years have made feasible the manufacturing of
2 operational spectral sun-photometers for environmental monitoring. The Precision Solar
3 Spectroradiometer (PSR), designed and manufactured at PMOD/WRC , Davos, Switzerland, is
4 one of the most accurate instruments of this class (Gröbner et al., 2012) . In this study we
5 have developed tools to retrieve IWV using PSR recordings, adopting two different
6 approaches; one using single wavelength channels and another retrieving from a wider
7 spectral region, the latter being impossible with filter radiometers. Retrievals in different
8 channels and spectral windows in the water vapor absorbing region of near infrared spectrum
9 were evaluated and selected. Both methods were applied to a 2-year long PSR dataset at the
10 German Meteorological Service (Deutscher Wetterdienst, DWD) site in Lindenberg, Germany
11 and results have been compared with sun-photometric (CIMEL), GPS, radiosonde and MWP
12 IWV datasets from the same station. Present study presents the technical details of all
13 instrumentation used, describes all the details of the development of this two methodological
14 approaches and estimates the uncertainties linked to them and finally all the comparisons for
15 the 2 year dataset are reported.

16

17 **2.Instrumentation**

18 Methodologies for retrieving IWV were applied to PSR measurements *at Meteorologisches*
19 *Observatorium Lindenberg – Richard Assmann Observatorium* (MOL-RAO) from the German
20 Meteorological Service “Deutscher Wetterdienst” (DWD) in Lindenberg (Tauche), in the
21 North-East Germany (52° 12' N, 14° 7' E), where a 2-year long PSR dataset is available (May
22 2014- April 2016). MOL-RAO is a supersite for measurements of aerology and radiation, thus
23 it provides a variety of collocated measurements that could be used for validation. MOL-RAO
24 is exclusively devoted to instrumental measurements of the atmosphere and a numerous
25 technical staff guarantees daily maintenance of the instruments. All instruments and
26 corresponding techniques are described below. Sunshine at the area ranges from 55
27 hours/month at December to 256 hours/month during summer months on average; also, rain
28 is recorded almost for 1/3 of days during all 12 months (Beyrich and Adam, 2005). Minimum
29 solar zenith angle (SZA) reaches 30° during summer months while during winter it is over 70°.
30 AOD is generally very low in the area, with maximum mean monthly values of 0.25 and 0.27
31 during June and July.

32

1 **2.1 PSR**

2 A new generation of solar spectroradiometer, the Precision Solar Spectroradiometer (PSR)
3 (Figure1) , is being developed at PMOD/WRC in order to eventually replace current filter sun-
4 photometers. It is based on a grating monochromator of stabilized temperature with a 1024
5 pixel Hamamatsu diode-array detector, operating in a hermetically sealed nitrogen-flushed
6 enclosure. The spectroradiometer is designed to measure the solar spectrum within the 300
7 to 1020 nm wavelength range with an average step of ~ 0.7 nm and spectral resolution from
8 1.5 nm to 6 nm (full width at half maximum, depending on the measured wavelength)
9 (Kouremeti and Gröbner, 2012). The design benefits from the experience gained from
10 successive generations of the successful Precision Filter Radiometers (PFR), including: an in-
11 built solar pointing sensor, an ambient pressure sensor and temperature sensors to provide
12 routine quality control information, which allows autonomous operation at remote sites with
13 state-of-the-art data exchange via Ethernet interfaces. The PSR used in this study is the
14 PSR#006, which is installed on the MOL-RAO site. This instrument has been calibrated at
15 PMOD/WRC using a 1000 W transfer standard lamp source, in May 2014 and October 2015.
16 A comparison between the two calibrations showed relative differences less than 1% for most
17 spectral channels and more than 2% only in the region above 980nm (Kouremeti et al. , 2015).
18 Moreover, stray light corrections have been applied and absolute direct and global
19 (horizontal) Irradiance time series are available for all 1024 available channels (Gröbner et al.,
20 2014). The cycle of routine measurements during this period was in a set of 5 Direct solar
21 Irradiance and 5 dark current measurements and average values for each pixel was saved at
22 1minute resolution. An evaluation of AOD retrievals from PSR have been performed during
23 the 4th Filter Radiometer Comparison (WMO, 2016, Kazadzis et al., 2018).



1

2 **Figure 1.** *PSR#004 and PSR#006 installed on a sun tracking device at MOL-RAO,*

3

4 **2.2 CIMEL Sun-photometer**

5 The CIMEL sun-photometer is a filter radiometer developed by Cimel Electronics (Paris,
6 France), which performs direct sun and sky radiance measurements. These measurements
7 are processed centrally and are widely available through Aerosol Robotic Network
8 (AERONET) (Holben et al., 1998). Measurements are performed at nine bandpass filters
9 between 340 and 1640 nm (8 of them dedicated to AOD retrieving and one used for IWV).
10 Direct measurements are performed usually every 10-15 minutes. Direct sun measurements
11 at 940 nm are used to retrieve IWV. At this channel the Full Width Half Maximum is 10nm,
12 (Schmid et al., 2001) which means that the solar signal recorded represents a relatively wide
13 spectral region. The method used to retrieve IWV is described in detail in Smirnov et al.
14 (2004). The principle of this method is to calculate a two constants' fit, using radiative transfer
15 model calculations in order to retrieve IWV from the transmittance recorded at 940 nm. The
16 precision of this retrieval was investigated by Alexandrov et al. (2009) who showed an error
17 in the region of 0.05-0.18cm depending on the amount of IWV.

18 The CIMEL Level 2 AOD data for MOL-RAO has been directly downloaded from AERONET
19 website (<https://aeronet.gsfc.nasa.gov/>). During the 2 years of this study, the station has
20 been equipped with three different instruments:

- 1 - Cimel CE318N, #787
- 2 - Cimel CE318N, #873 supplying #787 during its AERONET calibration
- 3 - Cimel CE318T (“Triple”) since October 2015, instrument of higher temporal resolution
- 4 (~ 1 minute)

5

6 **2.3 Global Positioning System**

7 GPS is a space based system that uses the signal transmitted from specific satellite
8 instrumentation in order to define the geolocation of ground based receivers. The signal
9 delays could be separated into dry (dependent on dry air gases) and wet (water vapor)
10 component. Although the biggest fraction of the delay is caused by the dry component, it is
11 estimated by hydrostatic equations, using the surface pressure, and subtracting it from the
12 total delay. This is considered a very accurate retrieval of the wet component, to which IWV
13 is directly proportional (Bevis et al, 1992). Wang et al. (2007) showed that the random error
14 of GPS IWV retrievals is in the order of 0.7 mm. GPS IWV retrievals are very valuable, since
15 this method could be applied to any receiver and obtain a very reliable and dense dataset of
16 frequent observations, both for daytime and night time, without being affected by cloud
17 conditions. Differences among GPS and sun-photometric retrievals are expected, as different
18 optical paths are used in each case and different air masses are detected: GPS path is a quasi-
19 random path depending on the position of the satellites while the sun-photometer path is
20 defined by the sun-instrument’s relative positions.

21

22 **2.4 Microwave Radiometer Profiler**

23 At MOL-RAO, a 22-channel MWP, MP-3000A /Radiometrics (Ware et al., 2003) provides
24 vertical temperature and humidity profiles. In principle, observations from these instruments
25 are based on recording the down-welling thermal emission of the atmosphere in the region
26 between 22 and 30 GHz, using a zenith sky looking sensor. A full description of the Water
27 Vapor retrieval methodology of MWP could be found at Westwater et al. (2005). Cadeddu et
28 al. (2013) have estimated the uncertainty of this technique in the order of 5% for IWV less
29 than 10mm.

30

31

32 **2.5 Meteorological Radiosonde**

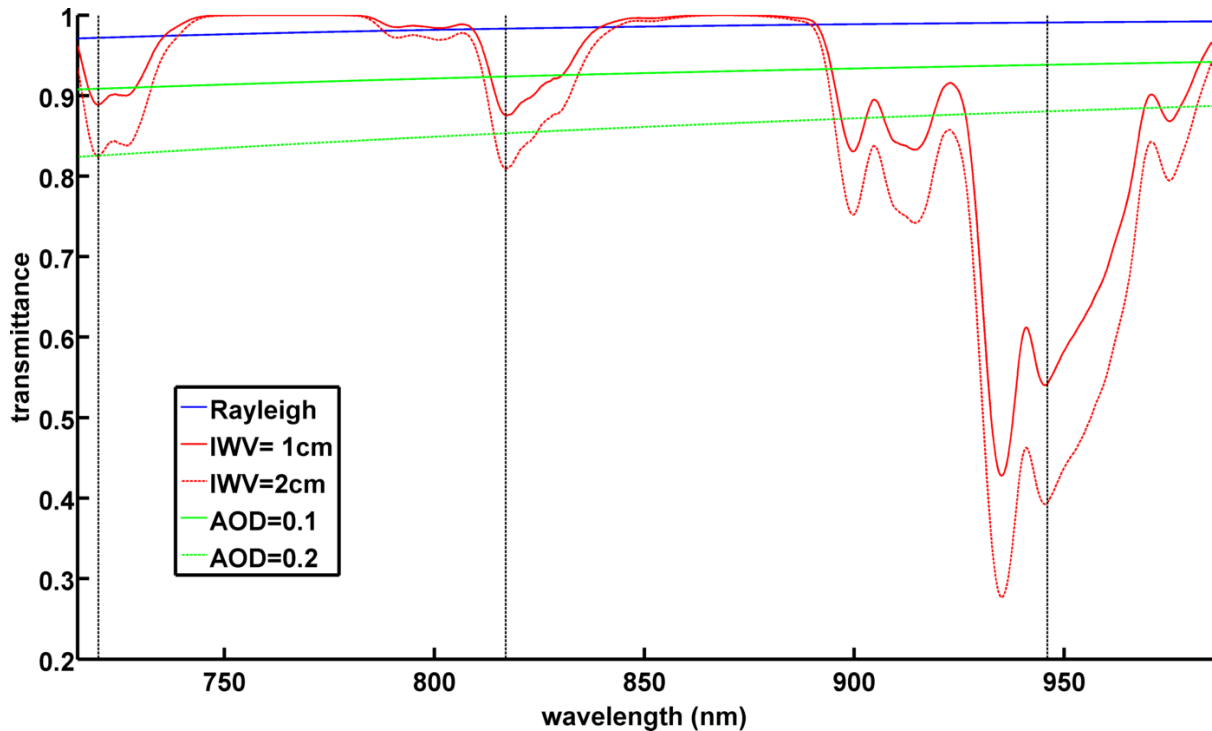
1 Meteorological radiosondes (RS) are launched in many places around the world, recording
2 vertical profiles of various meteorological variables (Temperature, Wind Speed, Humidity
3 etc). Water Vapor profiles provided by the soundings can be used to calculate IWV. This is the
4 most objective approach for validating ground based remote sensing techniques, since water
5 vapor is measured in-situ during the ascending procedure. Uncertainty for IWV retrieval in
6 this approach is introduced by the nature of the method, as the total ascending of a
7 radiosonde to stratosphere takes approximately an hour and also the path of the radiosonde
8 in the atmosphere is determined by winds; thus, it is not directly comparable to sun-
9 photometric estimations, which retrieve water vapor on the sun-point of observation optical
10 path. High uncertainties -up to 20%- for relative humidity, caused by warming due to sunlight
11 and thermal lag, have been reported (Pratt, 1985). Also, studies have reported differences
12 due to the use of different sensors (e.g. Soden and Lanzante 1996). Vaisalla RS92 radiosondes
13 are used in this study for which an uncertainty in the order of 5% for the RH (Relative
14 Humidity) measurements, during daytime in the Troposphere, has been reported
15 (Miloshevich et al.,2009). Radiosondes from MOL-RAO are launched 4 times per day (00h,
16 06h, 12h, 18h UTC). So, for this study 1-3 daytime soundings, per day, can be used, depending
17 on the season. Corrections, as suggested by Vömel et al. (2007) for the dependence of the
18 humidity sensor on temperature and radiation, were applied.

19

20 **3. Methodology**

21 In the near infrared measuring spectral region of PSR the most important water absorption
22 has been found in the 700-1000 nm wavelength region. Figure 2 shows the transmittance
23 from Rayleigh scattering, aerosols and IWV, as calculated by the MODerate resolution
24 atmospheric TRANsmisson Radiative Transfer Model (MODTRAN RTM) (Berk et al., 1987, Berk
25 et al., 1999). Aerosols direct effect on irradiance is measured through Aerosol Optical Depth
26 (AOD) which is the integrated extinction coefficient on vertical column due to aerosols.
27 Spectral variation of AOD at different wavelengths is measured through Ångström Exponent.
28 For the example on figure 2, Ångström Exponent equal to 1.5 was considered and aerosol of
29 AOD 0.1 and 0.2. Inclination of aerosol transmittance lines is proportional to Ångström
30 Exponent and higher AOD will lead to lower absolute values. WMO (2004) recommends 719,
31 817 and 946 nm central wavelengths to retrieve IWV, which appears as significant drops in
32 the solar transmittance spectra in Figure 2. Ingold et al. (2000) investigated the quality of the

1 retrievals at these wavelengths and found that the one at 946 nm is the most robust, which
 2 could be translated as the wavelength range with the strongest absorption of IWV.
 3 Considering that absorption of water vapor is higher in the 910-950 nm region, all calculations
 4 were performed for PSR channels in the spectral range.



5
 6
 7 **Figure 2.** *Transmittance of Water Vapor, Aerosols and Rayleigh scattering in the spectral*
 8 *region 700-1000 nm, calculated using MODTRAN set at 0.1 nm resolution, at SZA=0°*
 9 *IWV=1cm, IWV=2cm and AOD=0.1 and AOD=0.2 at 700nm using an Ångström Exponent of*
 10 *1.5. Black vertical dotted lines represent WMO recommendations for IWV retrieval.*

11
 12 **3.1 Monochromatic Approach**

13 The methodology in use is described in detail by Ingold et al. (2000) and it is the most
 14 common procedure to calculate IWV for sun-photometric devices using individual wavelength
 15 (filter) measurements. It is labeled as monochromatic in contrast to the second approach
 16 presented in Section 3.2, although it is calculated for a spectral region defined by the
 17 instrument's slit function or the limits of its bandpass filter.

18 The first step of the procedure is to calculate the Water Vapor transmittance T_w in the spectral
 19 window of use and afterwards to develop empirical formulas using RTM calculations to
 20 determine the IWV from the calculated transmittance.

1 For specific spectral regions in the near infrared, where absorption of dominant trace gases
 2 can be considered negligible, we can express the transmittance of the Atmosphere (T_{atmo}) as
 3 follows:

$$4 \quad T_{atmo} = \frac{I_{\lambda}}{I_{0,\lambda}} \quad (1)$$

6
 7 where I_{λ} is the recorded spectral irradiance at wavelength λ (in $Wm^{-2}nm^{-1}$) and $I_{0,\lambda}$ is the value
 8 of the solar irradiance at the top of the atmosphere at the same wavelength.

9 We can express the Beer-Lambert law (Swinehart, 1962) with respect to water vapor
 10 transmittance as follows:

$$11 \quad T_{atmo} = e^{(-m_{ray}\tau_{ray,\lambda} - m_a\tau_{a,\lambda})} * T_w \quad (2)$$

$$12 \quad T_w = \frac{I_{\lambda} e^{(m_{ray}\tau_{ray,\lambda} + m_a\tau_{a,\lambda})}}{I_{0,\lambda}} \quad (3)$$

13
 14 where T_w is the transmittance of water vapor, τ_{ray} is the Rayleigh scattering optical depth, τ_a
 15 is the aerosol optical depth (AOD), m is the relative optical air mass of aerosol and Rayleigh
 16 scattering accordingly. For the Rayleigh scattering cross-section we have used the formula
 17 found at Bodhaine et al. (1999).

18 Also, for $I_{0\lambda}$ we have used extraterrestrial values calculated for each of the PSR wavelengths
 19 measured as presented by Gröbner et. al. (2017a, 2017b). Spectral AODs were calculated
 20 using the Beer-Lambert law and the above extraterrestrial solar spectrum (Kouremeti and
 21 Gröbner, 2012). For calculating AOD at the wavelengths in the 920-950nm region, where
 22 direct sun measurements are affected by water vapor, we have applied a least square
 23 quadratic spectral extrapolation, using $\ln(\text{AOD})$ as function of $\ln(\text{wavelength})$ and the PSR
 24 AODs at 500 - 865 nm following Eck et al. (1999) suggestion for AERONET retrievals.

25 In order to convert T_w into IWV we have used the three-parameter expression found in Ingold
 26 et al. (2000):

$$27 \quad T_w = ce^{-a\chi^b} \quad (4)$$

1
2
3
4
5
6
7
8
9
10
11
12
13
14
15
16
17
18
19
20
21
22
23
24

where

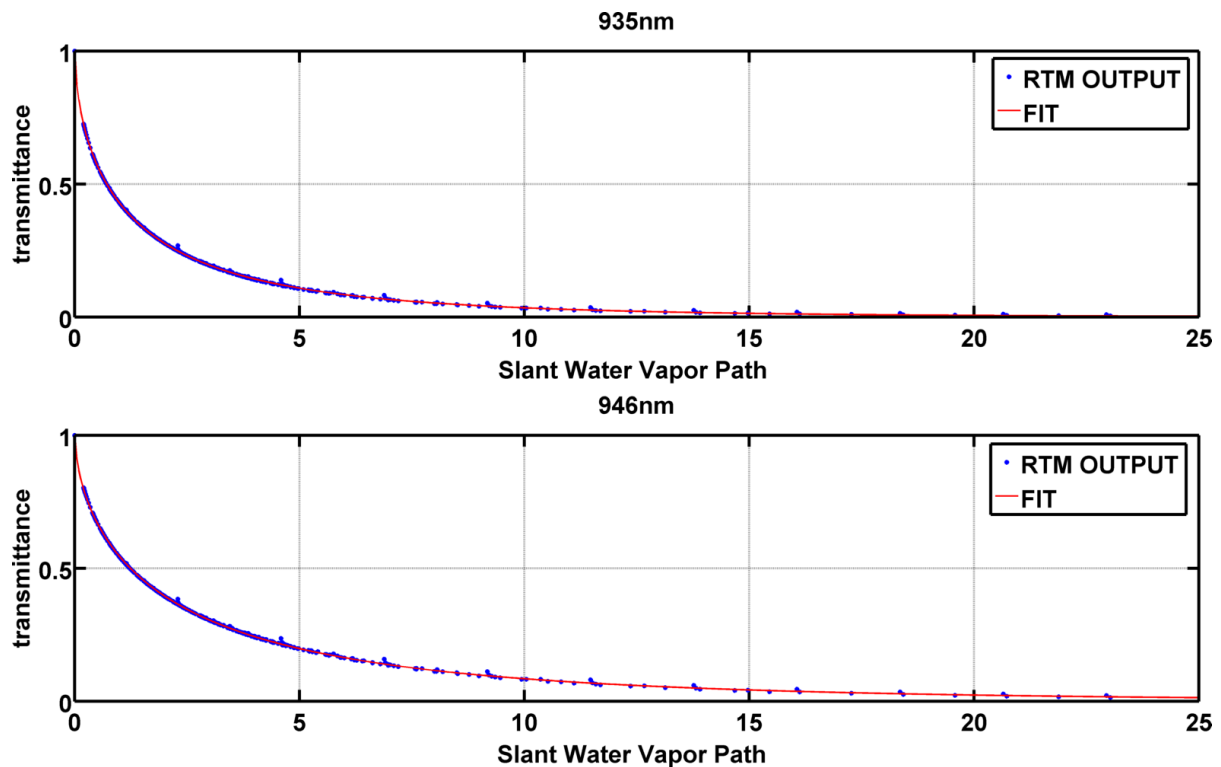
$$\chi = \frac{u m_w}{u_0} \quad (5)$$

with $u_0 = 10 \text{ kg/m}^2$, u representing IWV, m_w as the H_2O air mass and a, b, c the three wavelength dependent coefficients. At this step the coefficients of equation (4) can be estimated. For that purpose, we have used MODTRAN multiple runs for solar zenith angle (SZA) in the region of 0° to 85° with steps of 2.5° . We have used the mid-latitude built in model atmosphere, in the spectral region 0.7 to $1.0 \mu\text{m}$ and IWV from 0 to 40 mm with steps of 2 mm for site elevation set at 110m (MOL-RAO). The modeled spectra were convolved by the spectrally dependent instrument slit function in order to derive comparable (model-PSR) results. Then T_w retrieved from the output spectra was calculated as a function of Slant Water Vapor Path ($m_w * u$), and a fit of these values is used to estimate the coefficients (a, b, c) of equation (4). This procedure was repeated for all PSR channels in the whole spectral region of $900\text{-}950 \text{ nm}$. In figure 3, we present these fits for wavelengths 935.5 and 946 nm . Fits for wavelengths lower than 926 nm were unsatisfactory ($R^2 < 0.7$), suggesting that a different parameterization should be used in this area instead of equation (4).

After determining the coefficients a, b, c , equations could be solved in order to calculate the IWV :

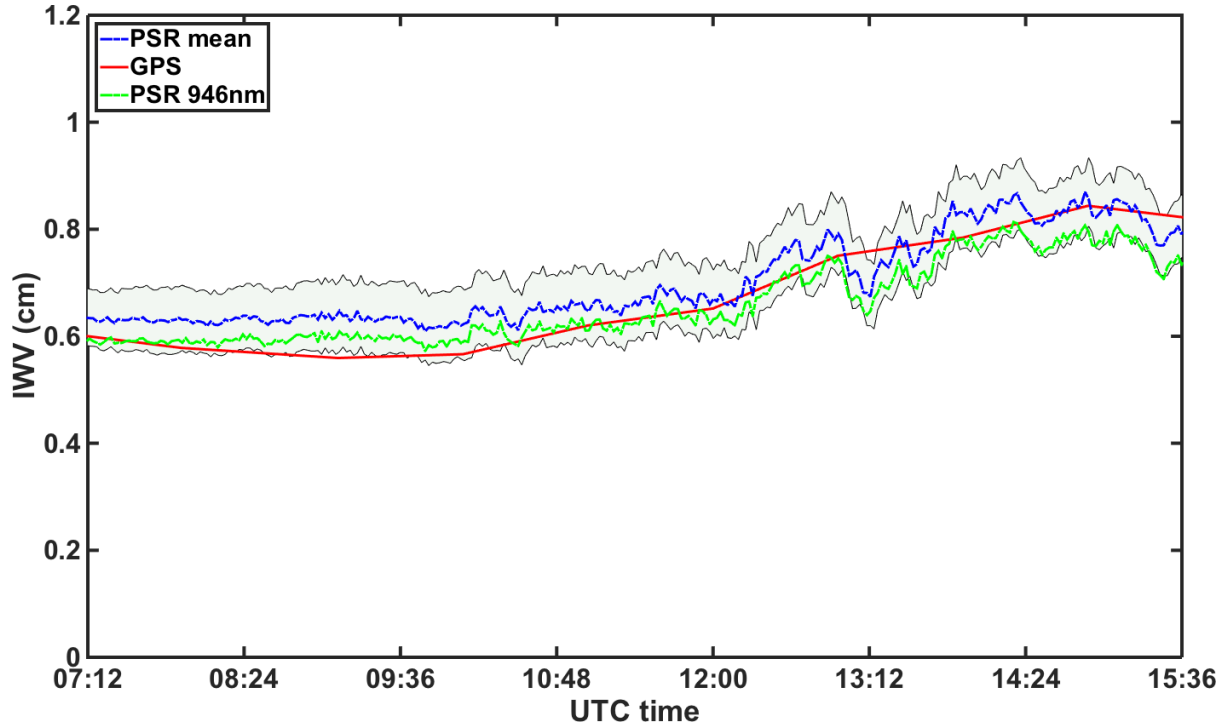
$$IWV = \frac{1}{m_w} \left(\frac{\ln(T_w/c)}{-a} \right)^{1/b} \quad (6)$$

Thus, IWV now depends only on T_w and air mass, although the coefficients depend on the altitude of the measurement site; so, different RTM runs are needed for each installation.



1
 2 **Figure 3.** Transmittance of IWV versus Slant Water Vapor Path ($m_w \cdot u$) calculated by
 3 MODTRAN, and three-parameters expression fit for 935 and 946nm bandpasses.

4
 5 In order to test the above methodology, we have retrieved IWV on September 30th, 2015, for
 6 each PSR channel in the 920-950 nm region separately, after calculating wavelength
 7 dependent a, b, and c coefficients. Also, aerosol and Rayleigh transmissions were calculated
 8 separately for each wavelength. The standard deviation of the residuals retrieved from
 9 different wavelengths is 0.11. The IWV retrievals at 946 and 935.5 nm have the smallest
 10 deviations compared to the GPS and CIMEL retrievals, because at these wavelengths the
 11 absorption due to water vapor absorption is higher. At these two wavelengths, the agreement
 12 with CIMEL measurements is very good, with correlations (expressed as the R^2 coefficient) of
 13 0.94 and 0.93 respectively. The lowest R^2 is found for wavelengths shorter than 928 nm which
 14 is in the order of 0.6. At figure 4 the mean IWV from all wavelengths for one day (30
 15 September 2015) is presented as an example, alongside with the standard deviation of all
 16 monochromatic retrievals and retrievals at 946 nm are presented as reference. The standard
 17 deviation of the residuals retrieved from different wavelengths is 0.11. Following WMO
 18 guidelines, we decided to use retrievals at 946 nm for this study and the monochromatic
 19 approach.



1
2 **Figure 4.** Retrievals of monochromatic approach on 30th September 2015 at various
3 wavelengths. Average IWV retrieved using the monochromatic approach at different
4 wavelengths represented by blue line; the shaded area represents the standard deviation (1σ)
5 of retrievals at different wavelengths, green line represent retrievals at suggested 946 nm and
6 the red curve represents the IWV retrieved from GPS.

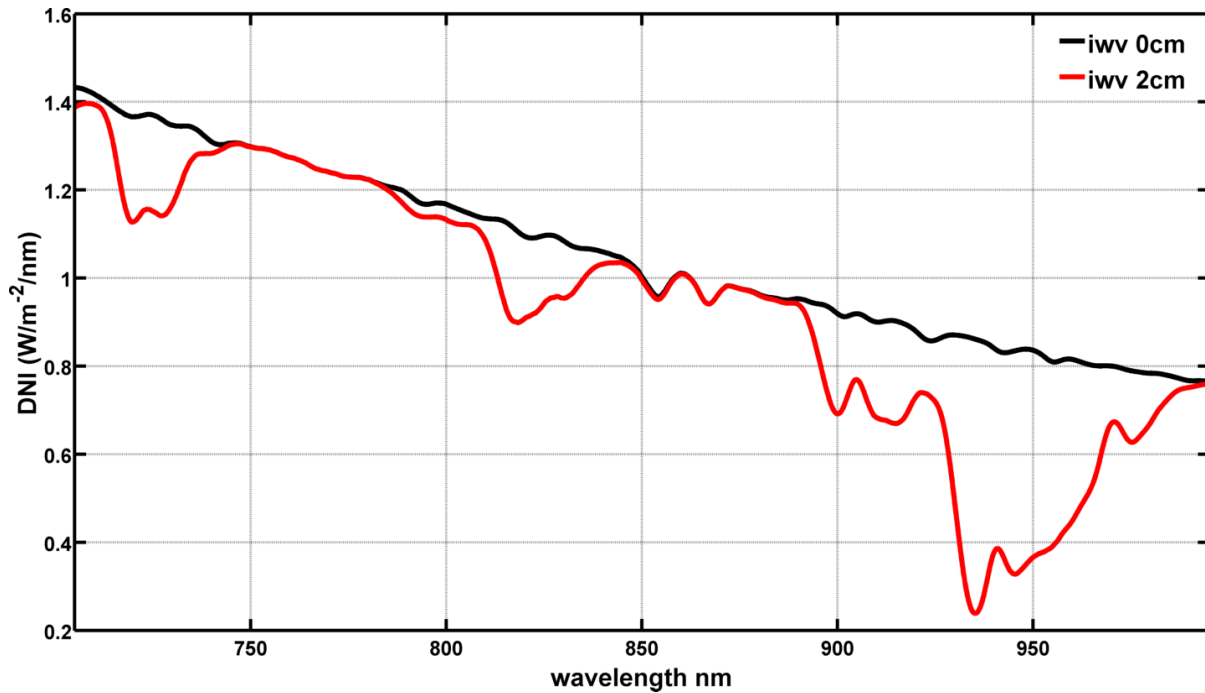
7 8 9 **3.2 IWV retrieval using integrated spectral windows**

10 In order to benefit from the high resolution spectral measurements available from the PSR
11 we developed a method that uses direct sun integrated irradiances for a spectral window in
12 contrast to individual/single wavelengths as previously described. This methodology is
13 expected to improve the IWV retrieval, since the large variability found in the IWV retrievals
14 at different wavelengths suggests that an approach that combines different wavelengths
15 could possibly be more accurate. Figure 5 shows two theoretical spectra in the region of 700-
16 1000 nm (calculated using MODTRAN), at SZA=0° with no aerosol load and with 0 and 2 cm
17 of IWV respectively. In this approach we have used the transmittance of the whole spectral
18 window, and then equation (3) can be written as follows:

19
$$T_{w,\Delta\lambda} = \frac{\int_{\lambda_1}^{\lambda_2} \frac{I(\lambda) \exp(m_{ray}\tau_{ray}(\lambda) + m_a\tau_a(\lambda))}{I_0(\lambda)} d\lambda}{\Delta\lambda} \quad (7)$$

1

2 Where λ_1 and λ_2 are the area wavelength limits, and $\Delta\lambda=\lambda_2-\lambda_1$.



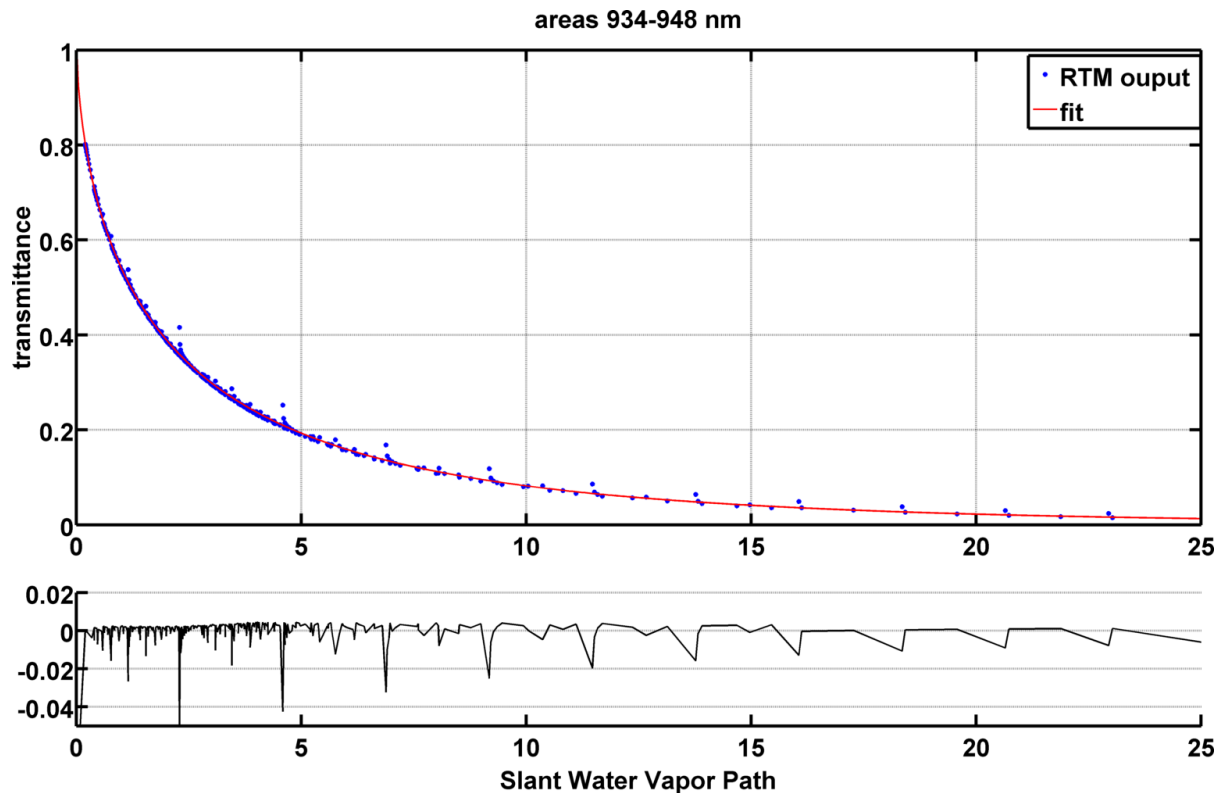
3

4 **Figure 5.** *Calculated Spectra of Direct Solar Irradiance, at SZA=0° with AOD=0 and IWV=0 cm*
5 *(black) and 2 cm (red), as calculated from MODTRAN 5.2.1 RTM.*

6

7 A similar methodology for converting transmittance to IWV, as in the monochromatic
8 approach described above is applied again in order to calculate a third order polynomial
9 function, valid for the wide spectral region. The same MODTRAN outputs were used as in the
10 monochromatic approach but integrated over each spectral window, and the coefficients for
11 equation (4) were calculated accordingly. Calculations have been performed for spectral
12 windows with variable wavelength limits. An investigation on the selection of spectral
13 window has been performed because, as monochromatic retrievals suggested (figure 4), the
14 IWV calculation depends on the wavelength region in use. This investigation was made by
15 changing the window, keeping the upper limit fixed at 948 nm and having the lower one
16 varying between 930 to 946 nm with a step of 1 nm. This selection was made based on the
17 water vapor absorption features as shown in Figure 5, so that the spectral window always
18 includes the high absorption region of 943-947 nm. Longer than 947 nm wavelengths were
19 avoided as there were higher uncertainties in the PSR calibration (Kouremeti et al., 2015,
20 Gröbner et al., 2017). As demonstrated in Figure 6 (for the 934 - 948 nm window), fitting of
21 the 3-parameter equation had results of similar statistics with the monochromatic approach

1 in that region. Residuals from fitting at this window are at average at 0.007 but there are also
 2 some up to 0.04. So, for each spectral window a new 3-parameter function is calculated.



3
 4 **Figure 6.** *Integrated Transmittance of IWV in the 934-948 nm window versus Slant Water*
 5 *Vapor Path ($m_w * u$) calculated by MODTRAN, and Third order polynomial fit.*

6
 7 In figure 7 results from different spectral windows have been compared to other instruments'
 8 retrievals for the whole MOL-RAO dataset. The coefficient of determination R^2 has been used
 9 to evaluate the performance of the spectral approach at different spectral windows, and was
 10 calculated as below:

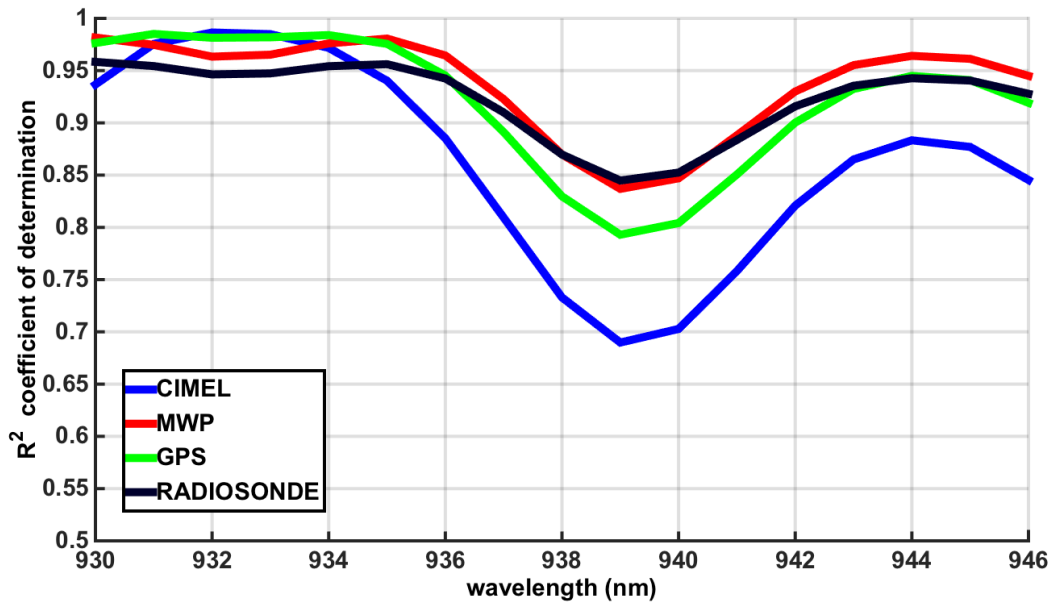
$$11 \quad R^2 = 1 - \frac{\sum_i (y_i - f_i)^2}{\sum_i (y_i - \langle y \rangle)^2} \quad (8)$$

12 where y_i are the IWV values from the other instruments (CIMEL, MW, GPS, RS), $\langle y \rangle$ is the
 13 average of those values and f_i are the IWV values from PSR.

14 Horizontal axis of figure 7 represents the lower limit of the spectral window, the higher being
 15 always fixed at 948 nm. The aim of this step is to find out which spectral window produces
 16 the more robust IWV retrieval results. These comparisons suggest that different spectral
 17 windows selection lead to different coefficients of determination for IWV retrieval compared
 18 with different instruments. However, results converge to defining a lower wavelength limit

1 between 932 and 936 nm, that will provide the best agreement for all the comparisons. The
 2 window 934-948 nm was selected to be used for further analysis, as a median of the above
 3 mention area.

4
 5



6
 7 **Figure 7**, IWV retrievals from PSR using spectral approach with different spectral windows,
 8 using fixed upper boundary at 946 nm and moving lower boundary at x axis, compared to
 9 synchronous ones of CIMEL, GPS, MWP and radiosonde, for the full 2-year measuring period.

10

11 It is interesting to observe different R² of the PSR IWV retrievals as compared using different
 12 instruments. Especially the fact that by minimizing the spectral window the R²s decrease
 13 showing a minimum of at window 939-946 nm. For this particular range all R²s are below
 14 0.85 with the one of CIMEL-PSR showing a minimum. The differences observed when
 15 comparing the PSR using different instruments can be partly explained based on the results
 16 of section 5.

17

18 **4. Uncertainty budget of IWV retrievals**

19

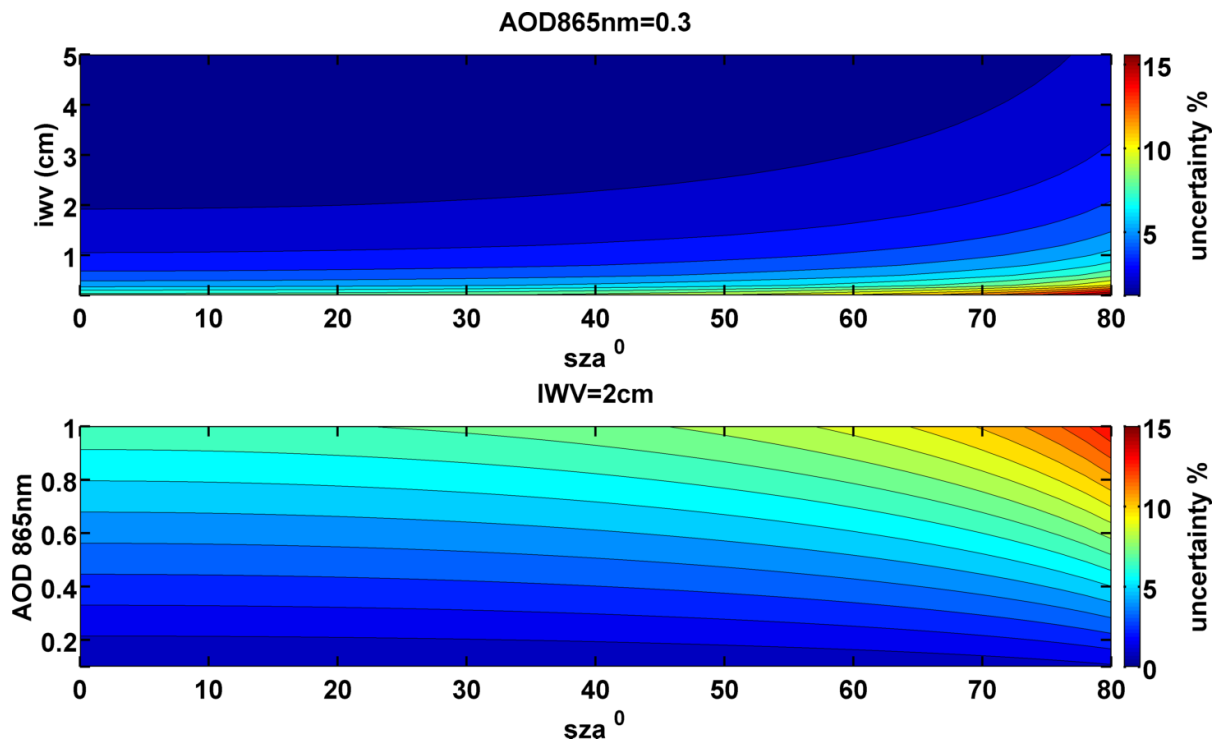
20 Uncertainty estimation of the IWV retrieval is very crucial for evaluating our comparison
 21 results. Beginning from equations (3) and (7) and the calculations of T_w , errors as introduced

1 from each variable are estimated and their propagation to the total uncertainty of IWV
2 retrieval is calculated.

$$3 \quad T_w = \frac{I_\lambda e^{(m_{ray}\tau_{ray,\lambda} + m_a\tau_{a,\lambda})}}{I_{0,\lambda}} \quad (3)$$

4
5
6 From equation (3), the term that introduces the higher uncertainty in the retrieval of the IWV
7 through the use of Beer-Lamber law is the AOD. A benefit from the methodology applied in
8 this case is that the same set of I_o are used for calculating T_w and AOD, and so errors related
9 to the determination of I_o do not propagate in the calculations. PSR AOD retrievals at 865 nm
10 have been found in accordance with prototype PFR triad when compared during FRC IV, 2015
11 (Filter Radiometer Comparison (GAW, 2016)) with average AOD differences at 865nm less
12 than 0.02. Also, a calibration stability study of the PSR was performed (Kouremeti et al., 2015)
13 and showed that the instrument was stable in the 2-year dataset of MOL-RAO, demonstrating
14 a mean difference of 0.3% with maximum of 4% in some channels. In addition, comparison
15 with different CIMEL instruments for longer periods in all cases showed differences smaller
16 than 0.03 at AOD at visible and near infrared wavelengths (Kouremeti and Gröbner, 2014).
17 So, the AOD related uncertainty calculated in all studies for the PSR is in at maximum 0.03.
18 Rayleigh optical depths in this spectral region are very low (~ 0.01 for 1000 mb pressure) and
19 the uncertainty is 1% (Teillet, 1990) and, thus, we may consider it negligible for the IWV
20 retrieval. Air masses were calculated using the formula found in Kasten (1966), which
21 assumes a standard vertical profile of humidity in the troposphere and introduces an error of
22 10% at SZA higher than 85° , due to variations in real atmospheric conditions but is negligible
23 for SZA lower than 75° (Tomasi et al., 1998).
24 Coefficients a, b, c derived from fitting of MODTRAN outputs introduce an uncertainty that is
25 related to the goodness of the calculated fit. For the monochromatic approach at 946nm,
26 Root Mean Square Error (RMSE) is 0.0021 and for the spectral approach at window 934-
27 948nm it is 0.0029. So, the uncertainties introduced using the empirical equation to estimate
28 IWV from T_w is 0.2% and 0.3% for each approach accordingly, due to the fitting.
29 Uncertainty is also introduced by the extrapolation of AOD from the 865 nm and lower
30 wavelength region to water absorbing wavelengths in the range of 934-948 nm. A sensitivity

1 analysis of the IWV retrieval in respect to fluctuations in AOD caused by the uncertainty of
 2 AOD was performed. The uncertainty of this extrapolation was calculated to be 0.03.
 3 Figure 8 shows the total expected uncertainty of IWV retrieval with respect to SZA, for the
 4 case of AOD=0.3 at 865 nm and the case of IWV equal to 2 cm. Highest uncertainties are
 5 expected for higher than 75° SZA, when IWV is very low or AOD very high. Very low IWV values
 6 could be found only at very dry atmospheres and even then, those are rarely below 0.2 cm.
 7 In the range of values found in the dataset of MOL-RAO (0.3 - 4.5cm), the maximum
 8 uncertainty is 0.28cm. For the 0.3 - 0.5cm values in our dataset, absolute uncertainty is
 9 calculated as 0.08-0.12 cm. Thus, the maximum expected uncertainty of the method, using
 10 PSR instruments, is found at the range of 15%, when the solar zenith angle is very high
 11 (SZA>75°) and AOD higher than 0.9.



12
 13 **figure 8.** Uncertainty (%) of IWV retrieved using monochromatic approach at 946 nm, for
 14 various Solar Zenith Angles (°) test figure, in respect to AOD (when IWV=2cm) in upper plot,
 15 and with respect to IWV (when AOD=0.3) in lower plot.

16
 17
 18
 19
 20

1 5. Results

2

3 In order to validate the results retrieved from both methodologies, we have used the various
4 IWV datasets recorded at MOL-RAO. Calculations have been performed for all PSR
5 measurements, but we have used only the ones synchronous to CIMEL level data in order to
6 avoid cloud contamination. So indirectly the AERONET cloud screening procedure (Smirnov
7 et al., 2000) has been used. For each CIMEL data point we have calculated the synchronous
8 PSR value by averaging all values in a ± 5 min interval. This approach produced a dataset of
9 3501 synchronous data points between PSR and CIMEL, 2507 between PSR and GPS and 2964
10 between PSR and MWP. For radiosondes, in order to have a robust coincidence criterion, we
11 have followed the approach of Schneider et al. (2010) averaging PSR measurements for ± 20
12 min from the time that the radiosonde reaches a 4 km height, in order to minimize spatial
13 and temporal PSR and radiosonde measurement differences.

14 For all the comparisons statistics are calculated for the differences

$$15 D_x = IWV_x - IWV_{PSR} \quad (9)$$

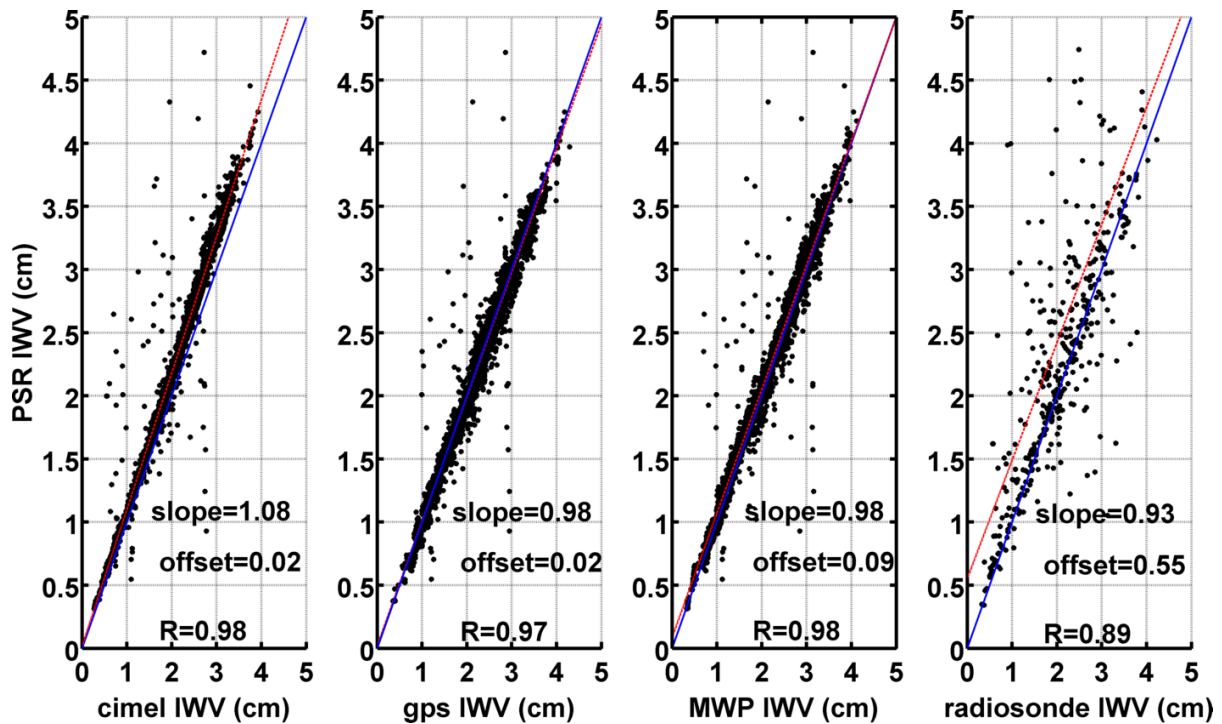
16 where x is the corresponding instrument/method, μ_x is the average value for D_x and

$$17 \sigma = \sqrt{\frac{\sum_1^N |D_{xi} - \mu_x|^2}{N-1}} \quad (10)$$

18 where N is the number of available, quality controlled observations.

19 For the monochromatic approach at 946 nm, the comparison is presented in Figure 9 and
20 corresponding statistics in Table 1. Better agreement was found when compared to MWP
21 retrievals, but at similar level as for the comparisons to CIMEL and to GPS retrievals. Mean
22 absolute difference is slightly lower when compared to GPS (0.01 cm), but the spread of the
23 differences is almost the same for CIMEL, GPS and MWP (standard deviation between 0.17
24 cm and 0.18 cm). Differences with CIMEL retrieval are within the CIMEL uncertainty range. It
25 appears that PSR overestimates the IWV compared to CIMEL for IWV larger than 3 cm, which
26 causes the different slope in the graphs. This feature is not shown in the comparison with GPS
27 and MWP at these IWV values. Schneider et al. (2010) also observed a different behavior of
28 CIMEL retrievals as compared to other methods, regarding dry or wet conditions in the
29 atmosphere and linked to filter characterization errors. Radiosonde retrievals had largest
30 deviations and more scattered differences, which is expected because of the different
31 temporal and spatial scale of the RS retrieval. Percentiles 10-90 of the differences are also

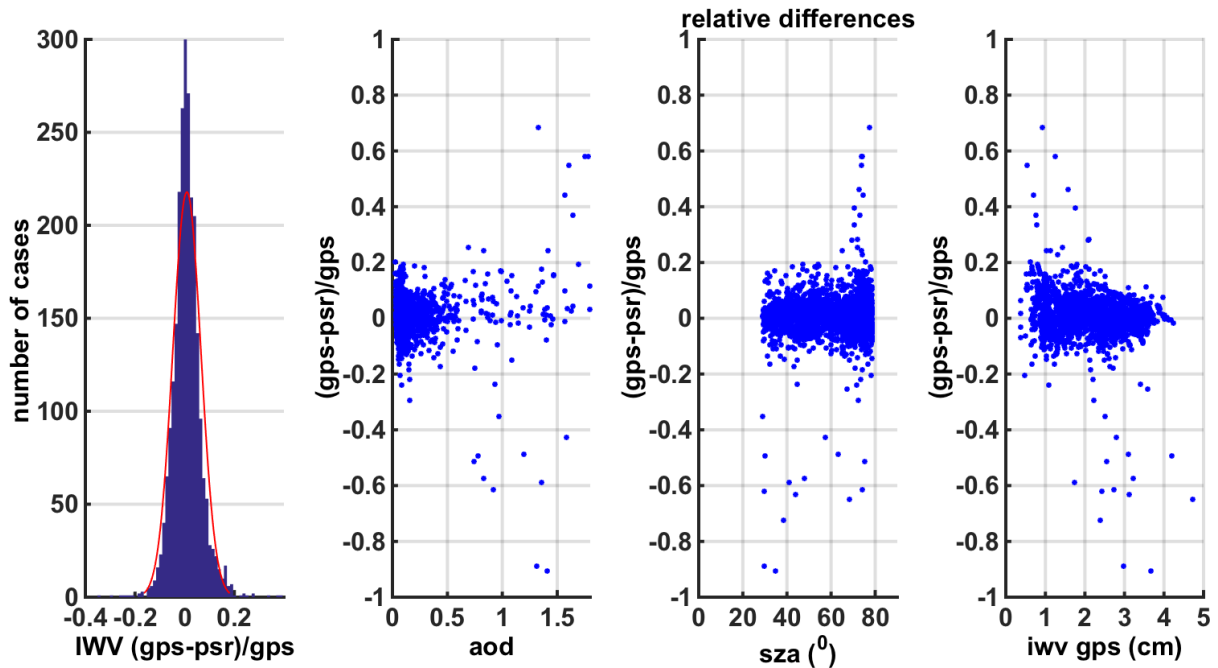
1 presented in table 1 and GPS, MWP and CIMEL retrievals have a spread of differences in the
 2 range of the uncertainties described for these instruments. In general RS retrievals
 3 demonstrate the most spread differences from the PSR retrievals, though the average and
 4 median are in the uncertainty range of the instruments. The high spread of the differences is
 5 explained by the random error introduced by the temporal variability of IWV in the time range
 6 averaged (± 20 min) and by the different paths of the sounding.



7
 8 **Figure 9:** IWV retrievals from PSR using monochromatic approach at 946 nm compared to
 9 synchronous ones of CIMEL, GPS, MWP and radiosonde, for the full 2-years measuring period.

10
 11 A histogram of relative difference of this retrieval compared to GPS is demonstrated in Figure
 12 10. Also, IWV retrievals relative differences are shown against other parameters (AOD, SZA
 13 and IWV from GPS). A normal distribution with mean at 0.024 cm and standard deviation of
 14 0.084 is fitted to the differences and passed the One-sample Kolmogorov-Smirnov test
 15 (Marsaglia et al., 2003). Thus 95% of the absolute differences are lower than 0.16cm. IWV
 16 differences against AOD at 865 nm show that almost all absolute relative differences higher
 17 than 0.2 cm (20%) are linked to AOD values higher than 0.5. This pattern could be connected
 18 to the larger uncertainty of AOD calculated by extrapolation at 946 nm, when AOD values are
 19 higher. Furthermore, it appears that most of the large differences appear at high SZA, but
 20 there are also some individual points showing large differences at lower SZA that could be

1 linked to AOD uncertainty. Compared to IWV retrieved from the GPS it appears that extreme
 2 differences are linked to overestimation from PSR when the absolute value is above 2 cm, and
 3 to underestimation when below , though GPS retrievals are not optimal at more dry
 4 conditions (Schneider et. al., 2010).

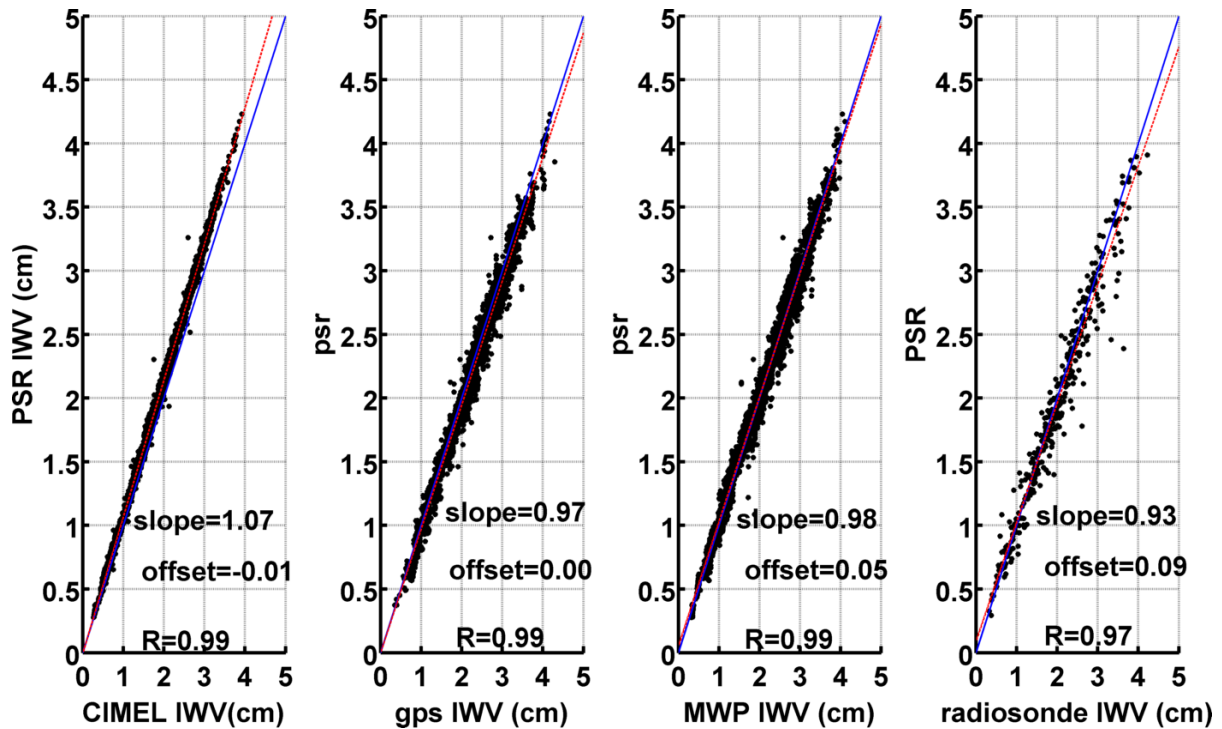


5
 6 **figure 10.** Histogram of *relative difference among synchronous GPS and PSR retrievals – using*
 7 *monochromatic approach at 946 nm- and plotted against AOD (retrieved from PSR at 865*
 8 *nm), solar zenith angle and IWV (retrieved from GPS).*

9
 10 Comparison of the PSR spectral method with other instruments is presented in Figure 11 and
 11 corresponding statistics in Table 2. It is clear that the spread of differences with all methods
 12 is significantly lower than for the monochromatic approach. All comparisons are found with
 13 R^2 between 0.96 and 0.98. CIMEL seems to underestimate, compared to this method, but also
 14 compared with the other instruments at higher IWV values. Although the slope caused by the
 15 overestimation is still presented in this approach, the spread of the differences among CIMEL
 16 and PSR retrievals is significantly lower than any other comparison, with $\sigma=0.07$ and 10-90
 17 percentiles of differences in a range of -0.23–0.02. Differences with GPS and MWP retrievals
 18 have the same spread and statistical behavior. Radiosonde data are in significantly better
 19 agreement with the spectral approach retrieval than with the monochromatic approach.
 20 Standard deviation of the differences is at least halved as compared to the monochromatic
 21 approach and all mean relative differences when compared to any other instrument are lower

1 than 0.7%. Comparison with RS' dataset has still significantly larger standard deviation than
 2 other comparisons but it is less than 1/4 of the the monochromatic approach's. Extreme
 3 values observed with the monochromatic approach are significantly reduced and the
 4 standard deviation is reduced to values from 0.07 for CIMEL to 0.18 for RS retrievals. A wider
 5 spread is observed at higher SZA, which is explained by the increase of the instrument related
 6 uncertainty at these angles.

7



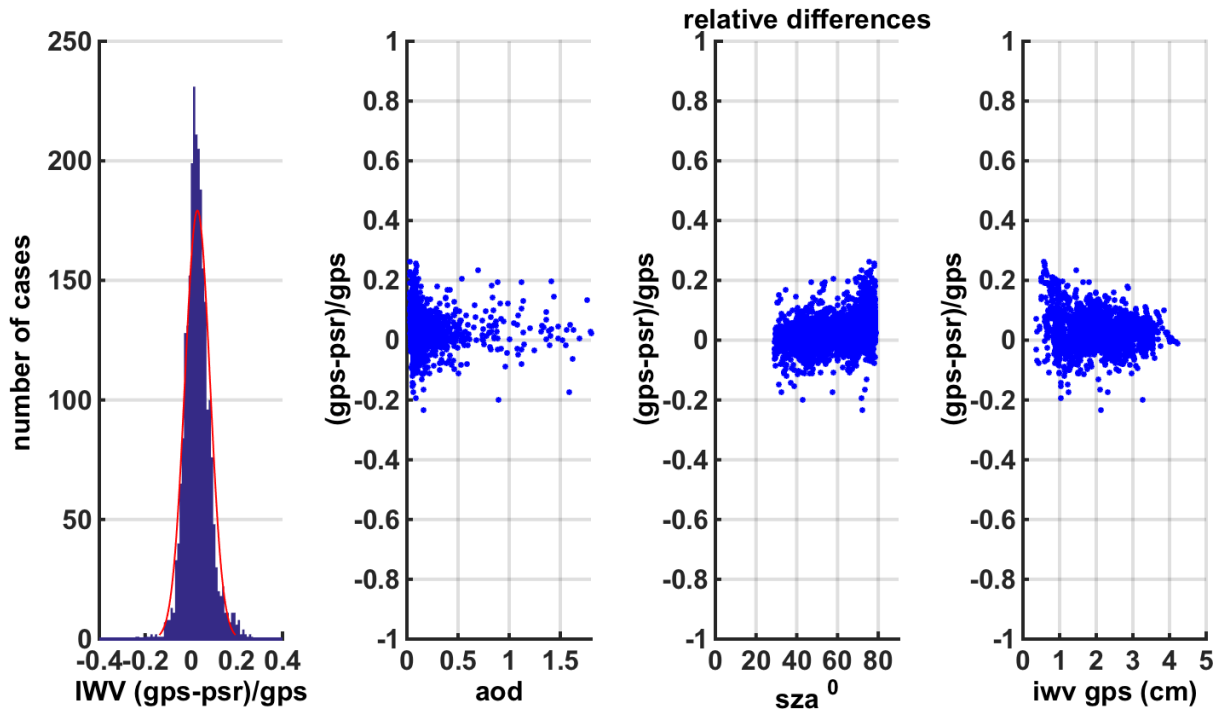
8

9 **Figure 11** IWV retrievals from PSR using spectral approach at 934-948 nm region, compared
 10 to synchronous ones of CIMEL, GPS, MWP and radiosonde, for the full 2-year measuring
 11 period.

12 Figure 12 displays a histogram of relative differences of the spectral approach for the spectral
 13 window 934-948 nm the GPS dataset and a relative IWV comparison against: AOD at 865nm,
 14 SZA and GPS' IWV. A normal distribution with mean at 0.021cm and σ at 0.042 is fitted at the
 15 data, passed the One-sample Kolmogorov-Smirnov test (Marsaglia et al., 2003) and 95% of
 16 differences are lower than 0.08 cm. The quality of spectral retrieval shows no dependence
 17 on absolute IWV values, as the distribution of differences in Figure 12 is independent of IWV.
 18 When the IWV relative difference is shown against AOD, higher relative differences than 0.1
 19 are more frequent for AOD lower than 0.2.

20

1



2

3 **figure 12.** *Relative difference among synchronous GPS and PSR retrievals – using spectral*
4 *approach at 934-948nm region- plotted against (a) AOD (retrieved from PSR at 865nm), (b)*
5 *solar zenith angle and (c) IWV (retrieved from GPS).*

6

7

8 **6. Conclusions**

9 The aim of this study was to develop methodologies and tools in order to retrieve IWV from
10 PSR spectral measurements. The methods which were developed can be applied to provide
11 long term time-series of IWV using any direct sun spectroradiometer able to measure at the
12 930-950 spectral range.

13 Two approaches to retrieve IWV from PSR spectral direct solar irradiance measurements
14 have been developed. The first one is the monochromatic approach using an individual
15 wavelength, and the second uses a spectral window. For both methods the corresponding
16 Water Vapor Transmittance has been retrieved from the PSR measurements, from which IWV
17 can be calculated using a three-parameter formula following the principles of Ingold's (2000)
18 work.

19 The dependence of the retrievals to other parameters has been investigated for both
20 approaches, and found to be affected in cases of low (<0.2) AOD coincidences. Larger

1 deviations were observed at high Solar Zenith Angles, which are linked to higher uncertainties
2 in those retrievals.

3 Comparisons to other instruments (CIMEL, MWP) and methods (GPS, radiosondes) have been
4 performed to select the optimum wavelength and spectral window for the IWV retrieval of
5 the PSR. All the channels in the infrared region of 900-950 nm were tested for
6 monochromatic approach and 946 nm bandpass was selected as giving significantly better
7 results than other channels. For the spectral approach all possible spectral windows limits
8 combinations were tested and the spectral window of 934-948 nm was finally chosen.

9 Uncertainties of the methodologies have been investigated and in more frequent
10 atmospheric conditions have been found less than 5%, while might reach up to 15% in cases
11 of very high AOD, very low IWV and SZA higher than 75° combined. In general, absolute
12 uncertainty is found to be in the range of 0.08-0.3 cm.

13 Retrievals from a 2-year long time-series at MOL-RAO in Lindenberg, Germany showed that
14 the monochromatic approach had differences in the order of 0.4% compared to GPS and
15 MWP, in the order of 2.7% compared to RS, and 3.3% compared to CIMEL. 95% of differences
16 with GPS retrievals are less than 0.15 cm.

17 Spectral approach's retrievals showed better agreement with other datasets, having
18 differences of 0.7% compared to CIMEL, 0.4% compared to GPS, 0.3% compared to MWP, and
19 0.5% when compared to RS. Also, the differences to other retrievals were always at least half
20 spread compared to monochromatic approach. Differences with GPS retrievals were less than
21 0.08cm in 95% of the dataset. Differences among the other instruments found independent
22 of other variables, suggesting robust appliance of the method.

23 Overall, the accuracy of IWV retrieval is in the same order of the other well established
24 methods and devices. The spectral approach, benefiting from the characteristics of PSR,
25 provided statistically better results. Also, having applied the method to a 2-year dataset,
26 indicated a stable long-term performance of the instrument, which shows that it can be used
27 for IWV calculations. The IWV method development and assessment presented in this work
28 provides an added value to the PSR instrument, being able to measure simultaneously
29 spectral solar irradiance components (direct and horizontal), aerosol spectral optical
30 properties (AOD, Angstrom Exponents) and IWV, constituting the PSR as a unique sun-
31 photometric instrument.

32

1 7.References

- 2 Alexandrov, M.D., Schmid, B., Turner, D.D., Cairns, B., Oinas, V., Laci, A.A., Gutman, S.I.,
3 Westwater, E.R., Smirnov, A. and Eilers, J., Columnar water vapor retrievals from
4 multifilter rotating shadowband radiometer data. *Journal of Geophysical Research:*
5 *Atmospheres*, 114(D2), 2009.
- 6 American Meteorological Society, Precipitable Water Vapor, *Glossary of Meteorology*, 2015.
- 7 Beyrich, F., and W. K. Adam, Site and Data Report for the Lindenberg Reference Site in CEOP
8 - Phase I. *Berichte des Deutschen Wetterdienstes*, 230, Offenbach am Main, Germany,
9 55 pp, 2007.
- 10 Berk, A., Bernstein, L.S. and Robertson, D.C., MODTRAN: A moderate resolution model for
11 LOWTRAN (No. SSI-TR-124). SPECTRAL SCIENCES INC BURLINGTON MA, 1987.
- 12 Berk, A., Anderson, G.P., Bernstein, L.S., Acharya, P.K., Dothe, H., Matthew, M.W., Adler-
13 Golden, S.M., Chetwynd Jr, J.H., Richtsmeier, S.C., Pukall, B. and Allred, C.L., MODTRAN
14 4 radiative transfer modeling for atmospheric correction. In *Proceedings of SPIE- The*
15 *International Society for Optical Engineering* (Vol. 3756, pp. 348-353),1999.
- 16 Bevis, M., S. Businger, T. A. Herring, C. Rocken, R. A. Anthes, and R. H. Ware. "GPS
17 Meteorology: Remote Sensing of Atmospheric Water Vapor Using the Global Positioning
18 System." *Journal of Geophysical Research*, Vol. 97, No. D14, , pp. 15,787-15,801, October
19 20, 1992
- 20 Bock, O., Bosser, P., Pacione, R., Nuret, M., Fourrié, N. and Parracho, A. : A high-quality
21 reprocessed ground-based GPS dataset for atmospheric process studies, radiosonde and
22 model evaluation, and reanalysis of HyMeX Special Observing 30 Period. *Q.J.R. Meteorol.*
23 *Soc.*, 142: 56–71. doi:10.1002/qj.2701, 2016.
- 24 Bodhaine, B. A., Wood, N. B., Dutton, E. G., and Slusser, J. R.: On Rayleigh optical depth
25 calculations, *J. Atmos. Ocean. Tech.*, 16(11), Part 2, pp 1854–1861, 1999.

- 1 Cadeddu, M. P., J. C. Liljegren, and D. D. Turner, The Atmospheric Radiation Measurement
2 (ARM) program network of microwave radiometers: Instrumentation, data and
3 retrievals, *Atmos. Meas. Tech.*, 6, 2359–2372, doi:10.5194/amt-6-2359-2013, 2013.
- 4 Campanelli, M., Estellés, V., Smyth, T., Tomasi, C., Martínez- Lozano, M. P., Claxton, B., Muller,
5 P., Pappalardo, G., Pietruczuk, A., Shanklin, J., Colwell, S., Wrench, C., Lupi, A., Mazzola,
6 M., Lanconelli, C., Vitale, V., Congeduti, F., Dionisi, D., and Cacciani, M.: Monitoring of
7 Eyjafjallajökull volcanic aerosol by the new European SkyRad users(ESR) sun-sky
8 radiometer network, *Atmos. Environ.*, 48, 33–45, 2012.
- 9 Campanelli, M., Mascitelli, A., Sanò, P., Diémoz, H., Estellés, V., Federico, S., Iannarelli, A. M.,
10 Fratarcangeli, F., Mazzoni, A., Realini, E., Crespi, M., Bock, O., Martínez-Lozano, J. A., and
11 Dietrich, S.: Precipitable water vapour content from ESR/SKYNET sun–sky radiometers:
12 validation against GNSS/GPS and AERONET over three different sites in Europe, *Atmos.*
13 *Meas. Tech.*, 11, 81-94, <https://doi.org/10.5194/amt-11-81-2018>, 2018.
- 14 Campanelli, M., Nakajima, T., Khatri, P., Takamura, T., Uchiyama, A., Estellés Leal, V., Liberti,
15 G.L. and Malvestuto, V., Retrieval of characteristic parameters for water vapour
16 transmittance in the development of ground based sun-sky radiometric measurements
17 of columnar water vapour. *Atmospheric Measurement Techniques*, 2014, num. 7, p.
18 1075-1087, 2014.
- 19 Che, H., Gui, K., Chen, Q., Zheng, Y., Yu, J., Sun, T., Zhang, X. and Shi, G., Calibration of the 936
20 nm water-vapor channel for the China aerosol remote sensing NETwork (CARSNET) and
21 the effect of the retrieval water-vapor on aerosol optical property over Beijing, China.
22 *Atmospheric Pollution Research*, 7(5), pp.743-753, 2016.
- 23 Eck, T. F., Holben, B. N., Ward, D. E., Mukelabai, M. M., Dubovik, O., Smirnov, A., Schafer, J. S.,
24 Hsu, N. C., Piketh, S. J., Queface, A., and Roux, J. L.: Variability of biomass burning aerosol
25 optical characteristics in southern Africa during the SAFARI 2000 dry season campaign
26 and a comparison of single scattering albedo estimates from radiometric measurements,
27 *J. Geophys. Res.-Atmos.*, 108, 2156–2202, doi:10.1029/2002JD002321, 2003.

- 1 Gröbner, J., Kazadzis, S., Kouremeti, N., Doppler, L., Tagirov, R. and Shapiro, A.I., February.
2 Spectral solar variations during the eclipse of March 20th, 2015 at two European sites.
3 In AIP Conference Proceedings (Vol. 1810, No. 1, p. 080008). AIP Publishing, 2017a.
- 4 Gröbner, J., Kröger, I., Egli, L., Hülsen, G., Riechelmann, S., and Sperfeld, P.: The high-
5 resolution extraterrestrial solar spectrum (QASUMEFTS) determined from ground-based
6 solar irradiance measurements, *Atmos. Meas. Tech.*, 10, 3375-3383,
7 <https://doi.org/10.5194/amt-10-3375-2017>, 2017b.
- 8 Gröbner, J., Kouremeti, N., Coulon, E., Durig, F., Gyo, M., Soder, R., Wasser, D.,
9 Spectroradiometer for Spectral Aerosol Optical Depth and Solar Irradiance
10 Measurements, annual report PMOD/WRC, page 13,
11 http://pmodwrc.ch/annual_report/2012_PMODWRC_Annual_Report.pdf, 2012.
- 12 Gröbner, J., Kouremeti, N., Nevas, S., Blattner, P., Characterisation Studies of Precision Solar
13 Spectroradiometer, PMOD-WRC Annual Report 2014, p26
14 http://pmodwrc.ch/annual_report/2014_PMODWRC_Annual_Report.pdf, 2014
- 15 Güldner, J.: A model-based approach to adjust microwave observations for operational
16 applications: results of a campaign at Munich Airport in winter 2011/2012, *Atmos. Meas.*
17 *Tech.*, 6, 2879-2891, doi:10.5194/amt-6-2879-2013, 2013.
- 18 Güldner, J. and Spänkuch, D., Remote sensing of the thermodynamic state of the atmospheric
19 boundary layer by ground-based microwave radiometry. *Journal of Atmospheric and*
20 *Oceanic Technology*, 18(6), pp.925-933, 2001.
- 21 GAW Report-No 231, Fourth WMO Filter Radiometer Comparison (FRC-IV) 28 September-16
22 October 2015; Davos, Switzerland,
23 https://library.wmo.int/opac/doc_num.php?explnum_id=3369, WMO, 2016
- 24 Halthore, R.N., Eck, T.F., Holben, B.N. and Markham, B.L., Sun photometric measurements
25 of atmospheric water vapor column abundance in the 940-nm band. *Journal of*
26 *Geophysical Research: Atmospheres*, 102(D4), pp.4343-4352, 1997.

- 1 Hartmann, D., Klein Tank, A., Rusticucci, M., Alexander, L., Brönnimann, S., Charabi, Y.,
2 Dentener, F., Dlugokencky, E., Easterling, D., Kaplan, A., Soden, B., Thorne, P., Wild, M.,
3 and Zhai, P.: Observations: Atmosphere and Surface, in: Climate Change 2013: The
4 Physical Science Basis. Contribution of Working Group I to the Fifth Assessment Report
5 of the Intergovernmental Panel on Climate Change, edited by Stocker, T., Qin, D.,
6 Plattner, G., Tignor, M., Allen, S., Boschung, J., Nauels, A., Xia, Y., Bex, V., and Midgley,
7 P., Cambridge University Press, Cambridge, United Kingdom and New York, NY, USA,
8 2013.
- 9 Hong L., Yunchanga C., Xiaominb W., Zhifangb X., Haishena W., Henga H., Meteorological
10 applications of precipitable water vapor measurements retrieved by the national GNSS
11 network of China, Geodesy and Geodynamics, vol 6 no 2, 135-142.
12 <http://dx.doi.org/10.1016/j.geog.2015.03.001>, 2015.
- 13 Holben, B.N., Eck, T.F., Slutsker, I., Tanre, D., Buis, J.P., Setzer, A., Vermote, E., Reagan, J.A.,
14 Kaufman, Y.J., Nakajima, T. and Lavenue, F., 1998. AERONET—A federated instrument
15 network and data archive for aerosol characterization. Remote sensing of environment,
16 66(1), pp.1-16.
- 17 Ingold, T., Schmid, B., Matzler, C., Demoulin, P., & Kampfer, N, Modeled and empirical
18 approaches for retrieving columnar water vapor from solar transmittance
19 measurements in the 0.72, 0.82, and 0.94 μm absorption bands. *Journal of*
20 *Geophysical Research.*, 105(D19), 24327–24343. <http://doi.org/10.1029/2000JD900392>,
21 2000.
- 22 Kasten, F., A new table and approximation formula for the relative optical air mass. Archiv für
23 Meteorologie, Geophysik und Bioklimatologie, Serie B, 14(2), pp.206-223, 1965 .
- 24 Kazadzis, S., Kouremeti, N., Diémoz, H., Gröbner, J., Forgan, B. W., Campanelli, M., Estellés,
25 V., Lantz, K., Michalsky, J., Carlund, T., Cuevas, E., Toledano, C., Becker, R., Nyeki, S.,
26 Kosmopoulos, P. G., Tatsiankou, V., Vuilleumier, L., Denn, F. M., Ohkawara, N., Ijima, O.,
27 Goloub, P., Raptis, P. I., Milner, M., Behrens, K., Barreto, A., Martucci, G., Hall, E., Wendell, J.,
28 Fabbri, B. E., and Wehrli, C.: Results from the 4th WMO Filter Radiometer Comparison for

1 aerosol optical depth measurements, *Atmos. Chem. Phys. Discuss.*,
2 <https://doi.org/10.5194/acp-2017-1105>, in review, 2017.

3 Kouremeti, N., Gröbner, J., Spectral Aerosol Optical Depth from a Precision
4 Spectroradiometer, PMOD-WRC Annual Report 2012, p33
5 http://pmodwrc.ch/annual_report/2012_PMODWRC_Annual_Report.pdf, 2012

6 Kouremeti, N., Gröbner, J., Spectral Aerosol Optical Depth From a Precision Solar
7 Spectroradiometer During Three Field Campaigns, PMOD-WRC Annual Report 2014, p30
8 http://pmodwrc.ch/annual_report/2014_PMODWRC_Annual_Report.pdf, 2014

9 Kouremeti, N., Gröbner, J., Doppler, L., Stability of the Precision Solar Spectroradiometer,
10 PMOD-WRC Annual Report 2015, p40
11 http://pmodwrc.ch/annual_report/2015_PMODWRC_Annual_Report.pdf, 2015

12 Marsaglia, G., W. Tsang, and J. Wang. "Evaluating Kolmogorov's Distribution." *Journal of*
13 *Statistical Software*. Vol. 8, Issue 18, 2003.

14 Miloshevich, L.M., Vömel, H., Whiteman, D.N. and Leblanc, T., Accuracy assessment and
15 correction of Vaisala RS92 radiosonde water vapor measurements. *Journal of*
16 *Geophysical Research: Atmospheres*, 114(D11), 2009

17 Nyeki, S., Vuilleumier, L., Morland, J., Bokoye, A., Viatte, P., Mätzler, C., & Kämpfer, N. , A 10-
18 year integrated atmospheric water vapor record using precision filter radiometers at two
19 high-alpine sites. *Geophysical Research Letters*, 32(23), 1–4,
20 <http://doi.org/10.1029/2005GL024079> , 2005.

21 Pratt, R.W., Review of radiosonde humidity and temperature errors. *Journal of Atmospheric*
22 *and Oceanic Technology*, 2(3), pp.404-407, 1985.

23 Reichard, J., U. Wandinger, M. Serwazi, and C. Weitkamp , Combined Raman lidar for aerosol,
24 ozone and moisture measurements, *Opt. Eng.*, 35, 1457–1465, 1996.

25 Schneider, M., Romero, P. M., Hase, F., Blumenstock, T., Cuevas, E., & Ramos, R., Continuous
26 quality assessment of atmospheric water vapour measurement techniques: FTIR, Cimel,

- 1 MFRSR, GPS, and Vaisala RS92. *Atmospheric Measurement Techniques*, 3(2), 323–338.
2 <http://doi.org/10.5194/amt-3-323-2010,2010>.
- 3 Schmid, B., Michalsky, J.J., Slater, D.W., Barnard, J.C., Halthore, R.N., Liljegren, J.C., Holben,
4 B.N., Eck, T.F., Livingston, J.M., Russell, P.B. and Ingold, T., Comparison of columnar
5 water-vapor measurements from solar transmittance methods. *Applied Optics*, 40(12),
6 pp.1886-1896, 2001.
- 7 Smirnov, A., Holben, B.N., Eck, T.F., Dubovik, O. and Slutsker, I., Cloud-screening and quality
8 control algorithms for the AERONET database. *Remote Sensing of Environment*, 73(3),
9 pp.337-349, 2000.
- 10 Smirnov, A, Holben, B.N., Lyapustin A., Slutsker, I. and Eck, T.F., AERONET processing
11 algorithms refinement, AERONET Workshop, El Arenosillo, Spain , May 10 - 14, 2004.
- 12 Soden, B.J. and Held, I.M., An assessment of climate feedbacks in coupled ocean–atmosphere
13 models. *Journal of Climate*, 19(14), pp.3, 2006.
- 14 Soden, B. J., and J. R. Lanzante, An assessment of satellite and radiosonde climatologies of
15 upper-tropospheric water vapor, *J. Climate*, 9, 1235–1250, 1996.
- 16 Swinehart, D.F., The beer-lambert law. *J. Chem. Educ*, 39(7), p.333 , 1962.
- 17 Teillet, P.M., Rayleigh optical depth comparisons from various sources. *Applied Optics*,
18 29(13), pp.1897-1900.354-3360, 1990.
- 19 Tomasi, C., Vitake, V. and De Santis, L.V., Relative optical mass functions for air, water vapour,
20 ozone and nitrogen dioxide in atmospheric models presenting different latitudinal and
21 seasonal conditions. *Meteorology and Atmospheric Physics*, 65(1), pp.11-30, 1998.
- 22 Vömel, H., Selkirk, H., Miloshevich, L., Valverde-Canossa, J., Valdés, J., Kyrö, E., Kivi, R., Stolz,
23 W., Peng, G. and Diaz, J.A., Radiation dry bias of the Vaisala RS92 humidity sensor.
24 *Journal of Atmospheric and Oceanic Technology*, 24(6), pp.953-963,2007.

- 1 Ware, R., Carpenter, R., Güldner, J., Liljegren, J., Nehr Korn, T., Sol-
2 heim, F.,
3 and Vandenberghe, F.: A multi-channel radiometric profiler of temperature, humidity
and cloud liquid, *Radio Sci.*, 38, 8079, doi:10.1029/2002RS002856, 2003.
- 4 Wang, J., Zhang, L., Dai, A., Van Hove, T., and Van Baelen, J.: A near-global, 2-hourly dataset
5 of atmospheric precipitable water from ground-based GPS measurements, *J. Geophys.*
6 *Res.*, 112, D11107, doi:10.1029/2006JD007529, 2007.
- 7 Westwater, E. R., Crewell, S., Mätzler, C., and Cimini, D.: Principles of surface-based
8 microwave and millimeter wave radiometric remote sensing of the troposphere,
9 *Quaderni della Società Italiana di Elettromagnetismo*, 1, 50–90, 2005.
- 10 WMO/GAW: Experts workshop on Global Surface-based Network for long term
11 observations of column aerosol optical properties, Davos, Switzerland, 8–10 March 2004.
12 GAW report No. 162, WMO TD No. 1287, 153 pp., available at:
13 <http://www.wmo.int/pages/prog/arep/gaw/gaw-reports.html> (last access: 21 October
14 2016), 2005,
- 15 WMO/GAW Report No. 231, The Fourth WMO Filter Radiometer Comparison (FRC-IV),
16 November 2016
- 17 Yu, S., Alapaty, K., Mathur, R., Pleim, J., Zhang, Y., Nolte, C., Eder, B., Foley, K. and Nagashima,
18 T., Attribution of the United States “warming hole”: Aerosol indirect effect and
19 precipitable water vapor. *Scientific reports*, 4, 2014.

1

2 *Table 1. Statistics of differences among retrievals from PSR using Monochromatic Approach*
3 *at 946 nm, and retrievals from other instruments for the whole dataset.*

	<i>N</i>	<i>MEAN</i> <i>(CM)</i>	<i>STANDARD</i> <i>DEVIATION(CM)</i>	<i>MEDIAN</i> <i>(CM)</i>	<i>PERCENTILE</i> <i>10-90 (CM)</i>	<i>MEAN RELATIVE (%)</i>	<i>R</i> ²
CIMEL	3501	-0.16	0.18	-0.14	-0.30 -0.04	-3.3	0.92
GPS	2507	0.01	0.17	0.01	-0.11 0.14	0.4	0.94
MWP	2964	-0.05	0.17	-0.04	-0.16 0.07	-0.4	0.95
RS	414	-0.41	1.03	-0.10	-1.42 0.22	-2.7	0.79

4

5

1 **Table 2.** Statistics of differences among retrievals from PSR using Spectral Approach at 934-
 2 948 nm window, and retrievals from other instruments for the whole dataset.

	<i>N</i>	<i>MEAN</i> (<i>CM</i>)	<i>STANDARD</i> <i>DEVIATION</i> (<i>CM</i>)	<i>MEDIAN</i> (<i>CM</i>)	<i>PERCENTILE</i> 10-90 (<i>CM</i>)	<i>MEAN RELATIVE</i> (%)	<i>R</i> ²
CIMEL	3501	-0.11	0.07	-0.10	-0.23 -0.02	-0.7	0.97
GPS	2507	0.05	0.10	0.04	-0.06 0.18	0.4	0.97
MWP	2964	-0.04	0.10	0.01	-0.12 0.12	0.3	0.98
RS	414	0.04	0.18	0.02	-0.13 0.25	0.5	0.95

3

4

1

2

3 Lexicon

4

AERONET	Aerosol RObotic NETwork
AOD	Aerosol Optical Depth
CIMEL	Sunphotometer Cimel CE318 used in AERONET network
DWD	Deutscher Wetterdienst (German Meteorological Service)
GPS	Global Positioning System
IWV	Integrated Water Vapor (water vapor column)
MODTRAN RTM	MODerate resolution atmospheric TRANsmisssion Radiative Transfer Model
MOL-RAO	Meteorologisches Observatorium Lindenberg – Richard Assmann Observatorium
MWP	Microwave Radiometer Profiler
PMOD/WRC	Physikalisch-Meteorologisches Observatorium Davos / World Radiation Center
PFR	Precision Filter Radiometer
PSR	Precision Solar spectroRadiometer
RH	Relative Humidity
RS	Meteorological Radiosondes
WMO	World Meteorological Organisation

5